Many-body enhanced nonlinear conductance resonance in quantum channels

Jong E. Han,[1,*] Saskia F. Fischer,[2,3,†] Sven S. Buchholz,[3] Ulrich Kunze,[3] Dirk Reuter,[4] Andreas D. Wieck,[4] and Jonathan P. Bird[5]

[1]*Department of Physics, State University of New York at Buffalo, Buffalo, New York 14260, USA*
[2]*Neue Materialien, Humboldt-Universität zu Berlin, D-12489 Berlin, Germany*
[3]*Werkstoffe und Nanoelektronik, Ruhr-Universität Bochum, D-44780 Bochum, Germany*
[4]*Angewandte Festkörperphysik, Ruhr-Universität Bochum, D-44780 Bochum, Germany*
[5]*Department of Electrical Engineering, State University of New York at Buffalo, Buffalo, New York 14260, USA*

We measure a strong enhancement of the nonlinear differential conductance ($g = dI/dV$), the amplitude of which exceeds the universal quantum conductance ($2e^2/h$), under finite bias voltage in quantum point contacts (QPCs). By developing a spin-based model in the low-electron-density limit, we demonstrate that this resonance is an intrinsic nonequilibrium phenomenon that arises from many-body induced modifications to the QPC potential. A comparison with the linear conductance ($G = I/V$) shows that this phenomenon is driven by many-body dynamics within a single one-dimensional sub-band.

PACS number(s): 73.21.Hb, 73.23.Ad, 73.63.Nm, 85.35.Be

The well-known quantization of the conductance[1,2] of quasi-one-dimensional (1D) quantum point contacts (QPCs) and quantum wires (QWRs), in integer units of $G_0(=2e^2/h)$, can be described within a single-particle picture in the Landauer-Buttiker formalism.[3,4] At the same time, however, many-body phenomena, including those that involve spin-based interactions, have been widely suggested to modify the conductance in the limit where the carrier density is lowered sufficiently that many-body energy terms dominate over the carrier kinetic energy (for reviews, see Refs. 5–7, and for various theoretical models, see Refs. 8–14). Recently, a strong conductance enhancement beyond G_0 was observed in the nonlinear transport of QWRs, when their transport was governed by a single 1D sub-band.[15,16] Although many-body effects were proposed as the origin of this enhancement, it remains unclear precisely what nonequilibrium mechanism can drive such a drastic departure from the quantized conductance. Here we provide a scenario that explains this behavior in terms of nonequilibrium transport due to spin fluctuations in quasi-1D constrictions. From diagrammatic calculations, it is shown that correlations of the spin fluctuations strongly modify the effective potential barrier (E_b) formed in the 1D QWR, and it is this effect that yields the observed nonlinear conductance enhancement.

The phenomenon that we are interested in explaining is demonstrated here with results for two GaAs/AlGaAs QPCs [which we refer to here as QPCs A and B, see the inset to Fig. 1(a) for the geometry], fabricated by nanolithography and wet etching. QPCs were defined with nominal lengths and widths of about 100 nm and had a global Ti/Au top gate that covered the reservoirs and the QPC. A two-dimensional electron gas (2DEG) was located 55 nm below the top surface and had (in the dark at 4.2 K) a carrier density, mobility, and mean free path of 3.1×10^{11} cm^{-2}, 1×10^6 cm^2/Vs, and 9.5 μm, respectively. Differential conductance ($g = dI/dV_{sd}$) was measured by use of the lock-in technique, superimposing a dc source-drain bias (V_{sd}) on top of a small ac excitation. Measurements were made in a dilution refrigerator for temperatures of 0.02–10 K. In rough dc bias measurement

scans five of nine QPCs showed immediate evidence for a conductance peak, with two of these exhibiting a peak with $g > G_0$. The reproducibility of our results was demonstrated in several cooling cycles, performed over the course of a year. As illustrated in Fig. 1(a), in the limit $V_{sd} \rightarrow 0$, the differential conductance showed flat quantized plateaus indicating the high quality of these constrictions. As the top-gate voltage (V_g) is increased, the onset of conduction is followed by the well-known 0.7 feature.[5] The 1D sub-band energy spacings were determined from the transconductance (dg/dV_g) derived from g[17] measured as a function of both V_g and V_{sd}. Typical values for the separation of the first and second sub-bands ($\Delta E_{1,2}$) were around 10 meV, significantly larger than the values (1–3 meV) typically reported for split-gate QPCs. The large subband spacing is critical for the nonlinear experiments here, since it allows us to apply dc bias without inducing transport via higher sub-bands.

The resonant enhancement of the QPC conductance under nonlinear bias is demonstrated in Fig. 1(b). Here we plot high-resolution measurements of $g(V_{sd})$ for a series of V_g close to pinch-off. For the lowest conductance curves, it is clear that an increase of V_{sd} to 4 mV yields a rapid increase of g to a value beyond G_0. Related behavior was found previously in the experiment of Morimoto *et al.*,[15,16] who showed that this resonant enhancement became more pronounced with increasing channel length, a result that we return to explain below. It is clear from Fig. 1(b) that the resonance is seen only for a narrow range of V_g close to pinch-off and that it is rapidly suppressed with increase of the background g. This can also be seen in the colorscale plot of $g(V_g, V_{sd})$ in Fig. 1(c). Values of g exceeding G_0 are plotted in dark red and the width of the resonances is very narrow, about 400 μV. For increasing gate voltage, as the background conductance increases toward the right-hand side of the contour, the resonances are suppressed. As a further illustration of the range of the resonance, in Fig. 1(a) we compare the gate-voltage dependence of the differential conductance, measured with $V_{sd} = 0$ to that for $V_{sd} = 4$ mV. The data are similar to those in Ref. 15 and show that the
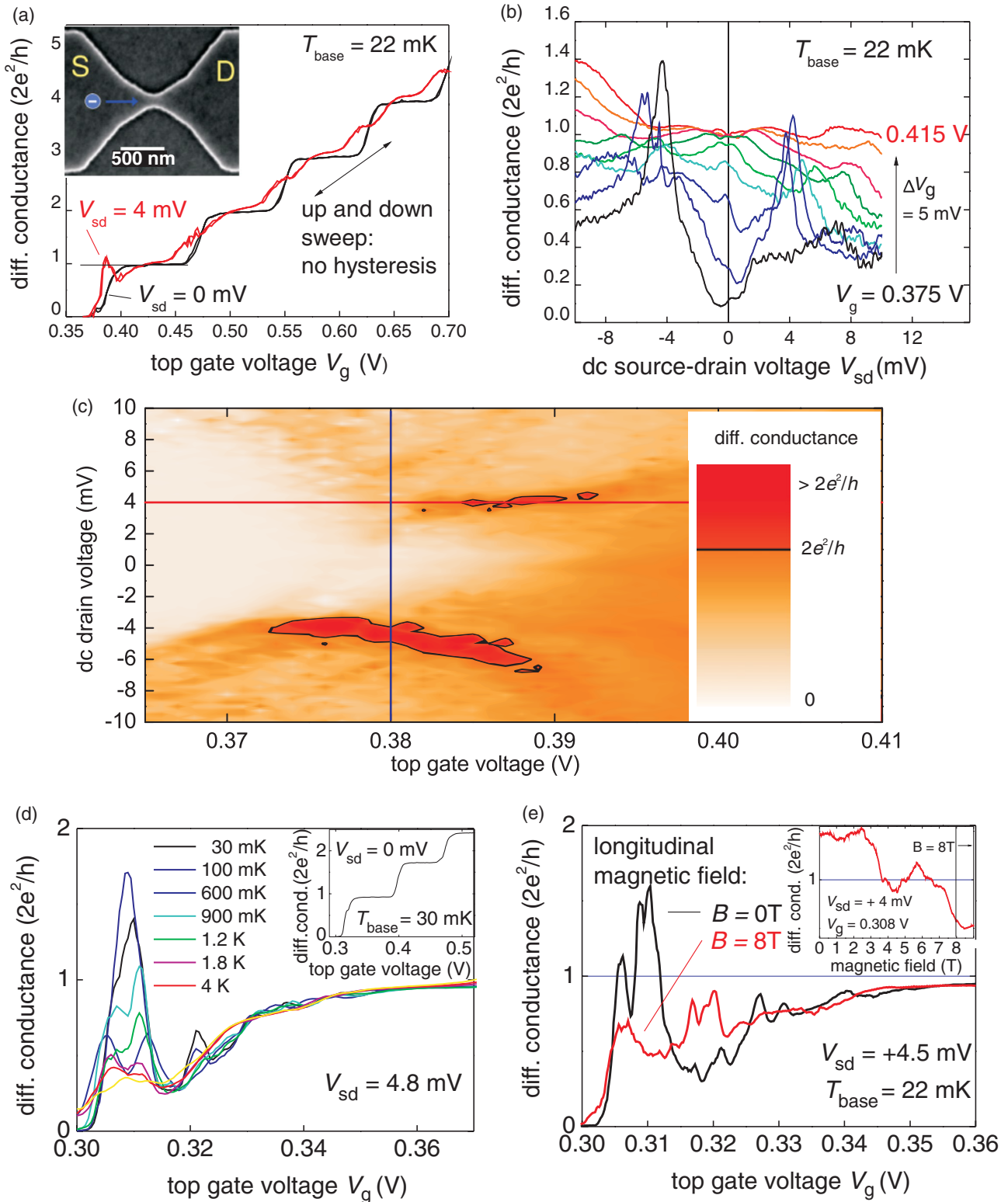
FIG. 1. (Color online) (a) $g = dI/dV_{sd}$ measured vs. V_g (up and down sweeps) for $V_{sd} = 0$ and $V_{sd} = +4$ mV at 22 mK, QPC A. (Inset) Typical QPC before deposition of the top gate. (b) $g(V_{sd})$ measured at different V_g, showing $g > G_0$, QPC A. (c) Color plot of $g(V_{sd}, V_g)$. $g > G_0$ values in red. (Red line) $g(V_{sd} = +4$ mV) of (a), (blue line) $g(V_g = 0.38V)$ of (b), QPC A. (d) Temperature dependence of the conductance peak, QPC B. (Inset) Linear conductance showing the 0.7 anomaly. (e) Nonlinear conductance peak for $V_{sd} = +4.5$ mV at $B = 0$ T and 8 T, QPC B.

enhancement of the conductance above G_0 is associated with the threshold for a single sub-band. Sweeping V_g up and down

shows that the resonance is highly reproducible and that there is no hysteresis. We have, furthermore, found the resonance
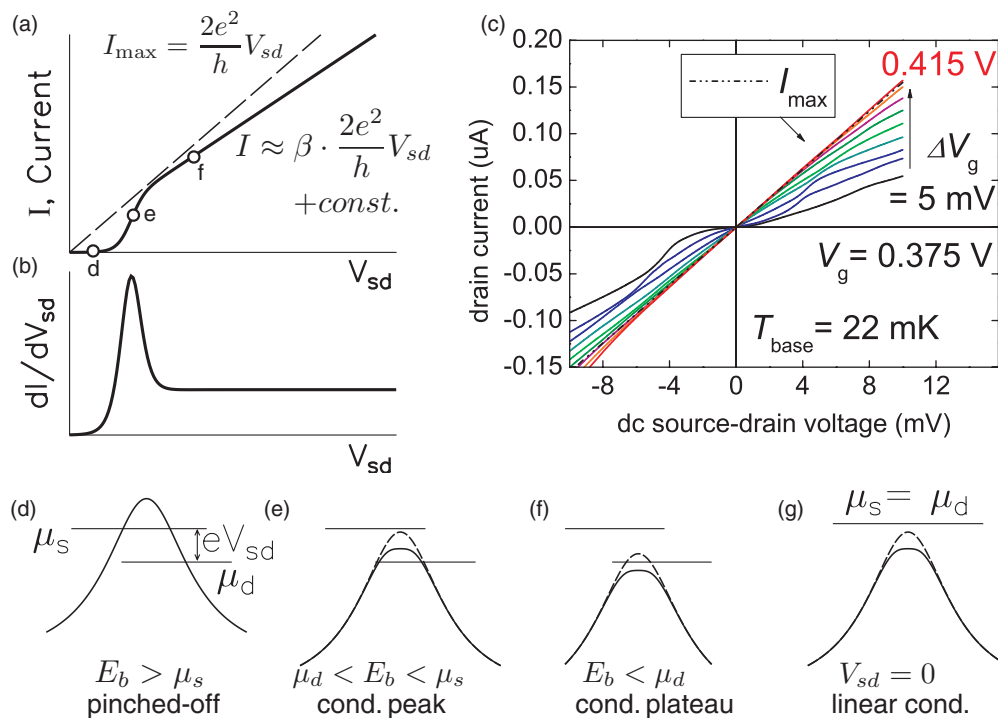
FIG. 2. (Color online) (a) Schematic I-V_{sd} relation. As a pinched-off QPC [in (d)] becomes conducting [in (e)] the potential barrier shifts downward (dashed to solid curve) due to the energy gain via coupling to spin fluctuations and the current becomes enhanced. The current should be bound by the maximum current, $I_{max} = G_0 V_{sd}$, if only one sub-band is responsible. Once the conductance saturates [in (f)], the potential shift does not affect the plateau. (b) Corresponding differential conductance. (c) Measured I-V_{sd} curves. [(d)–(f)] Energy configurations at different gate voltages. E_b is the potential barrier height. (g) Linear-conductance regime.

to be stable with regards to variation of the ac excitation (4–240 μV rms).

Two further features of the resonance that should be addressed concern its temperature and magnetic-field dependence, which are demonstrated in Figs. 1(d) and 1(e). Consistent with Ref. 15, the resonance is suppressed quickly with increase of temperature beyond 1 K [Fig. 1(d)]. Such behavior is, therefore, opposite to that reported for the 0.7 feature,[5] whose visibility typically improves above 1 K, suggesting that the resonance arises from a different mechanism. In Fig. 1(e) we show that a large in-plane magnetic field suppresses the resonance, similar to the trend reported by Morimoto et $al.$[15] The inset to this figure reveals an interesting behavior that is observed by first configuring V_g to achieve maximal resonance at $B = 0$ T and then increasing the magnetic field while holding V_g fixed. g reduces in a steplike manner, from an enhanced value of more than G_0 to around G_0, near 4 T, and then to a value close to zero.

To begin our discussion of the theoretical interpretation of the observed phenomena, we first explain the nonlinear conductance peak heuristically as follows. For given V_{sd}, the current through a single 1D sub-band is given by $I = \frac{2e}{\hbar} \int_{-k_d}^{k_s} \frac{dk}{2\pi} v_g(k, V_{sd}) = \frac{2e^2}{\hbar} V_{sd}$ with $\mu_{s,d}$ and $k_{s,d}$ the chemical potentials and Fermi wave vectors, respectively, for the source (s) and drain (d) reservoirs. This formula applies for $E_b < \min(\mu_d, \mu_s)$ [see Fig. 2(d)] even when the potential barrier or the group velocity $v_g(k, V_{sd})$ is modified by many-body effects. When E_b lies inside the chemical potential window [$\mu_d < E_b < \mu_s$; see Fig. 2(e)] the relation is modified to

$I = 2e/h(\mu_s - E_b)$, in the limit of perfect transmission. If the bias dependence of the barrier is ignored, the differential conductance becomes $g = dI/dV = \beta G_0$ with the parameter β being the fractional voltage drop between the source and the constriction. In infinitely-long QWRs, the shift of the bottom of the band can be absorbed in the chemical potential and is often ignored. However, in QPCs the change of potential near the constriction should be carefully taken into account. In the strongly interacting limit near pinch-off, the finite electron density in the constriction changes the electronic structure and $E_b(V_{sd})$ may develop a strong bias dependence. As the bias increases by δV_{sd}, the electron density in the constriction increases, leading to stronger many-body effects, which, in turn, induces a second-order downward shift of the potential barrier by δE_b. Under such conditions, the current should exhibit an abrupt change near pinch-off as depicted in Fig. 2(a). The current increase δI can be expressed as $\delta I = \frac{2e}{\hbar}[\beta e \delta V_{sd} + \delta E_b]$. $\delta E_b / \delta V_{sd}$ is model-dependent and there is no limit to its magnitude a $priori$. When $\delta E_b / \delta V_{sd}$ becomes large enough, the maximum differential conductance

$$g_{max} = G_0 \left(\beta + \frac{1}{e} \frac{\partial E_b}{\partial V_{sd}} \right) \qquad (1)$$

may exceed G_0, just as measured in our experiment. In the linear-transport regime, [$\mu_d = \mu_s$, see Fig. 2(g)], the condition $\mu_d < E_b < \mu_s$ is never satisfied and the single-sub-band differential conductance is bounded by G_0, even though the many-body effect may be present in E_b.

Confirmation that the resonance arises from only a single 1D sub-band can be obtained by examining the QPC I-V curves. With a single sub-band, the current should be bounded by $I_{max} = G_0 V_{sd}$ [dashed line in Fig. 2(a)], regardless of many-body effects. This is demonstrated experimentally in Fig. 2(c), which shows I-V curves obtained by numerical integration of the differential conductance of Fig. 1(b). The curves are clearly bounded by I_{max}, and a similar conclusion may be reached from the data of Morimoto *et al.*[16] Thus, the resonance in the differential conductance does indeed appear to arise from many-body effects taking place in a single 1D sub-band. Such character explains why the large 1D sub-band spacing in our devices aids the observation of the resonance. Hints of collective behavior of itinerant electrons under strong lateral confinement have been given earlier in Ref. 18.

Moving beyond this heuristic description to quantitatively account for the experiment, we have developed a phenomenological model that takes account of spin fluctuations of itinerant electrons in a quasi-1D system.[19,20] We start with an electron gas discretized on a noninteracting chain with the Hamiltonian given by the tight-binding model

$$\mathcal{H}_0 = \sum_{i=-\infty}^{\infty} \sum_{\sigma} \left\{ -t_0(c_{i+1,\sigma}^\dagger c_{i\sigma} + c_{i,\sigma}^\dagger c_{i+1\sigma}) + \left[V(x_i) - \mu - \frac{1}{2} g\mu_B \sigma H \right] n_{i\sigma} \right\}, \quad (2)$$

with the gate potential $V(x_i) = V_g[\cosh(x_i/L_g)^\alpha]^{-2}$ on the i-th point x_i along the transport direction. The parameter α is introduced here to allow variation of the potential shape from quadratic ($\alpha = 1$) to flatter ($\alpha > 1$) forms, thus mimicking constrictions of different lengths. $c_{i\sigma}^\dagger$ is the electron creation operator of spin index $\sigma = \pm 1$, the electron occupation $n_{i\sigma} = c_{i\sigma}^\dagger c_{i\sigma}$, t_0 is the hopping integral, and H is the external Zeeman field. The free electron g factor has been used in the calculation. To connect to experiment, the length of the gate potential in the transport direction is chosen as $L_g = 240$ nm, with the discretization spacing $\Delta x = L_g/32 = 7.5$ nm. This leads to the hopping integral $t_0 = \hbar^2/(2m\Delta x^2) \approx 10$ meV with the effective mass $m \approx 0.067m_e$ in GaAs. This discretization sets the coarse-grain length scale for our model of long-wavelength limit.

For the inter-electron interaction, we consider the Heisenberg spin-exchange model

$$\mathcal{H}_{int} = \frac{1}{2} \sum_{i=-N}^{N} J_i (\hat{\mathbf{S}}_i - \hat{\mathbf{S}}_{i+1})^2, \quad (3)$$

where the spin of *itinerant* electrons at interacting sites $i = -N, \ldots, N$ ($N = 30$) is given by $\hat{S}_{i\alpha} = \frac{1}{2} \sum_{\beta\gamma} c_{i\beta}^\dagger \sigma_{\beta\gamma}^\alpha c_{i\gamma}$ with the Pauli matrix σ^α ($\alpha = x, y, z$). Positive spin-exchange coupling J_i induces ferromagnetic coupling between itinerant electrons nearby. For numerical calculations, we attenuate the coupling constant adiabatically with the same width as the gate potential, $J_i = J_0[\cosh(x_i/L_g)]^{-2}$. The spin coupling contributes to a negative shift of the barrier when incoming electron spins dynamically align with the spin fluctuation[19,20] near the barrier. This effect becomes sensitive in the low-density limit near pinch-off when the effective kinetic energy competes with many-body interaction. With the barrier between the source-drain chemical potentials under finite bias, such abrupt change in the electronic structure leads to the enhancement of the conductance as discussed for Eq. (1).

The model is numerically solved by the nonequilibrium Keldysh Green function technique[21] with the self-energy calculated to second order of interaction. Figure 3 confirms the picture discussed earlier. In Fig. 3(a), differential conductance curves at finite source-drain bias $V_{sd} = 1$ meV show a peak exceeding G_0. (V_{PO} denotes the pinch-off gate voltage by the noninteracting limit.) Here the spin-coupling parameter J_0 is treated as a free parameter. Once J_0 exceeds 11 meV, the conductance peak grows rapidly. In the linear transport regime ($V_{sd} = 0$ meV), the conductance is bounded by G_0 as shown in Fig. 3(b). It is interesting that the calculations carried to the first-order mean-field approximation (dash-dotted line) show only a conductance step at $g = \beta G_0$, as discussed earlier. This illustrates that the resonant conductance occurs due to the coupling of quantum fluctuations with itinerant electrons near a QPC constriction. In principle, bosonic fluctuation models other than that considered here could also generate similar resonant conductance physics. Quantitative comparisons to experimental temperature and magnetic field dependence will determine the applicability of the models.

At $J_0 = 12.5$ meV, the strong temperature dependence in Fig. 3(c) reproduces the experimental temperature scale for suppression of the resonance. Note that the characteristic energy scale of 2.9 K is much smaller than any other energy parameters in the model, as is typical for emergent many-body phenomena. Calculations performed with nonzero magnetic field also confirm the reduction of conductance peak for $H > 4$ T, and the progression of the peak position to more-negative gate voltage at high fields.[15]

Increasing the constriction length via the QPC potential yields a remarkable enhancement of the conductance peak, as we show in Fig. 3(d). In this figure, the potential shape (inset) has been changed from a quadratic [$\alpha = 1$, below Eq. (2)] profile to a flatter form by increment of $\Delta \alpha = 0.2$. This results in a growth of the effective region over which the spin-coupling becomes pronounced, hence leading to enhanced conductance peaks. As the QPC gets even longer, the effective region does not grow due to a voltage slope in the potential [see the inset of Fig. 3(d)], while the resonant many-body state becomes more extended. This leads to reduced coupling and eventual reduction of the conductance peak. The overall agreement of our model with experiment (both here and in Refs. 15 and 16) offers important insight into the origins of the nonlinear resonance. In our devices here, the large 1D sub-band spacing promotes a strongly 1D character to transport, while in the experiment of Morimoto *et al.*[15] this was achieved by studying long QPCs, with a large length-to-width ratio.

In conclusion, we have developed a quantitative many-body theory that captures the resonant enhancement of the nonlinear conductance in QPCs in the lowest one-dimensional sub-band. Key to this phenomenon is the ability of quantum fluctuations to induce a significant modification of the constriction potential, over a narrow range of gate voltage. Due to the strong magnetic field dependence, models with itinerant spins are likely candidates, as confirmed by performing calculations
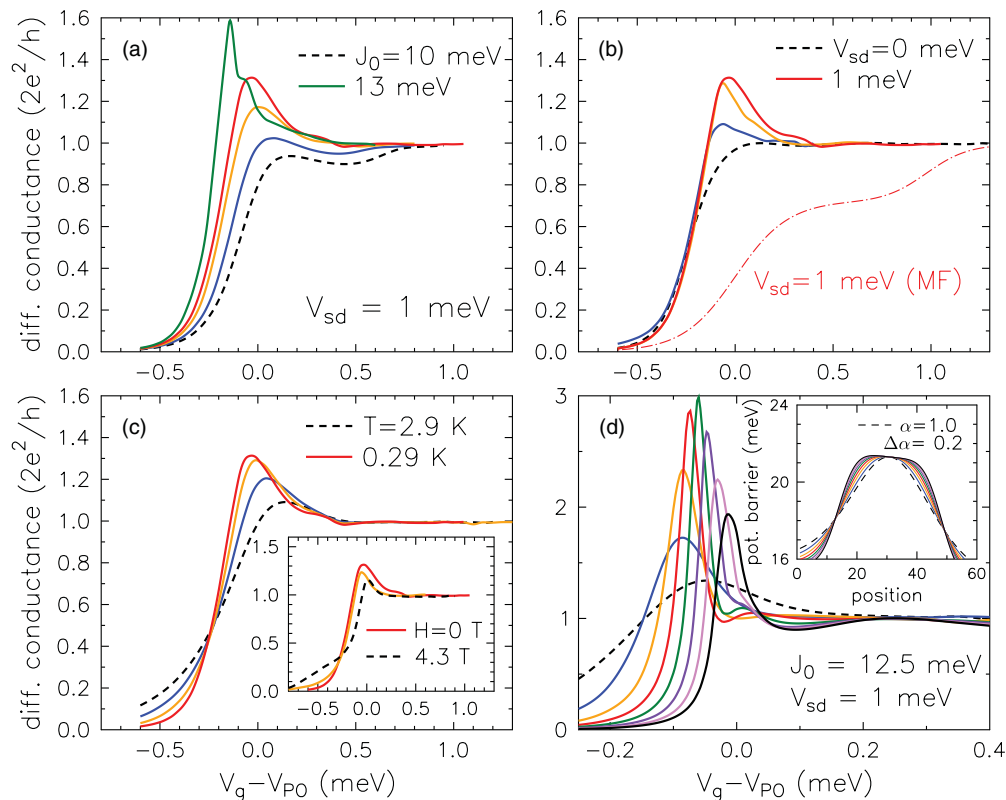
FIG. 3. (Color online) (a) Calculated g at finite bias $V_{sd} = 1$ mV with several spin-coupling constants J_0. $J_0 = 10, 11, 12, 12.5, 13$ meV from bottom to top curves. (b) g at several V_{sd} $(0, 0.25, 0.5, 1$ meV from bottom to top) for $J_0 = 12.5$ meV. Absence of conductance peak in the mean-field approximation (dash-dotted red curve) demonstrates the importance of spin fluctuations. (c) The conductance peak with strong temperature and magnetic field (inset) dependence within the experimental range. $J_0 = 12.5$ meV; $V_{sd} = 1$ meV. (d) Strong enhancement of conductance peak for flatter potential barrier (inset). Increment of α is 0.2 [defined below Eq. (2)].

of spin fluctuations in the low-density limit as an example. Our experimental results confirm the ideas of our model, showing that, in the limit of large sub-band spacing, the conductance (I/V) remains bounded below G_0, even though the differential conductance can significantly exceed this. Our study, therefore, shows that nonequilibrium transport can reveal new many-body energetics that is essential to a full understanding of QPC/QWR systems.

*jonghan@buffalo.edu

†sfischer@physik.hu-berlin.de

[1]B. J. van Wees, H. van Houten, C. W. J. Beenakker, J. G. Williamson, L. P. Kouwenhoven, D. van der Marel, and C. T. Foxon, Phys. Rev. Lett. **60**, 848 (1988).

[2]D. A. Wharam, T. J. Thornton, R. Newbury, M. Pepper, H. Ahmed, J. E. F. Frost, D. G. Hasko, D. C. Peacock, D. A. Ritchie, and G. A. C. Jones, J. Phys. C **21**, L209 (1988).

[3]R. Landauer, IBM J. Res. Dev. **1**, 223 (1957); **32**, 306 (1988).

[4]M. Büttiker, Phys. Rev. Lett. **57**, 1761 (1986).

[5]Special issue: J. P. Bird and M. Pepper (eds.), J. Phys.: Cond. Matt. **20**, 16 (2008).

[6]A. P. Micolich, J. Phys. Condens. Matter **23**, 443201 (2011).

[7]J. P. Bird and Y. Ochiai, Science **303**, 1621 (2004).

[8]H. Bruus, V. V. Cheianov, and K. Flensberg, Physica E **10**, 97 (2001).

[9]K.-F. Berggren and I. I. Yakimenko, Phys. Rev. B **66**, 085323 (2002).

[10]Y. Meir, K. Hirose, and N. S. Wingreen, Phys. Rev. Lett. **89**, 196802 (2002).

[11]D. J. Reilly, Phys. Rev. B **72**, 033309 (2005).

[12]T. Rejec and Y. Meir, Nature **442**, 900 (2006).

[13]A. D. Güçlü, C. J. Umrigar, H. Jiang, and H. U. Baranger, Phys. Rev. B **80**, 201302(R) (2009).

[14]T. Song and K.-H. Ahn, Phys. Rev. Lett. **106**, 057203 (2011).

[15]T. Morimoto, M. Henmi, R. Naito, K. Tsubaki, N. Aoki, J. P. Bird, and Y. Ochiai, Phys. Rev. Lett. **97**, 096801 (2006).

[16]T. Morimoto, N. Yumoto, Y. Ujiie, N. Aoki, J. P. Bird, and Y. Ochiai, J. Phys. Condens. Matter **20**, 164209 (2008).

[17]S. F. Fischer, G. Apetrii, S. Skaberna, U. Kunze, D. Reuter, and A. D. Wieck, Appl. Phys. Lett. **81**, 2779 (2002).

[18]R. D. Tscheuschner and A. D. Wieck, Superlattices Microstruct. **20**, 615 (1996).

[19]K. Aryanpour and J. E. Han, Phys. Rev. Lett. **102**, 056805 (2009).

[20]Y. Tokurar and A. Khaetskii, Physica E **12**, 711 (2002).

[21]L. V. Keldysh, JETP **20**, 1018 (1965).